Title
Structure of the cholera toxin secretion channel in its closed state

Journal
Nature Structural & Molecular Biology, 17(10)

ISSN
1545-9993

Authors
Reichow, Steve L
Korotkov, Konstantin V
Hol, Wim GJ
et al.

Publication Date
2010-10-01

DOI
10.1038/nsmb.1910

Peer reviewed

HHS Public Access

Author manuscript

Nat Struct Mol Biol. Author manuscript; available in PMC 2011 April 01.

Published in final edited form as:

Nat Struct Mol Biol. 2010 October ; 17(10): 1226–1232. doi:10.1038/nsmb.1910.

Structure of the cholera toxin secretion channel in its closed state

Steve L. Reichow[1,3], **Konstantin V. Korotkov**[1,3], **Wim G. J. Hol**[1,$], and **Tamir Gonen**[1,2,$]

[1] Department of Biochemistry, University of Washington, Seattle WA 98195, USA

[2] Howard Hughes Medical Institute, University of Washington, Seattle WA 98195, USA

Abstract

The type II secretion system (T2SS) is a macromolecular complex spanning the inner and outer membranes of Gram-negative bacteria. Remarkably, the T2SS secretes folded proteins including multimeric assemblies like cholera toxin and heat-labile enterotoxin from *Vibrio cholerae* and enterotoxigenic *Escherichia coli*, respectively. The major outer membrane T2SS protein is the "secretin" GspD. Electron cryomicroscopy reconstruction of the *V. cholerae* secretin at 19 Å resolution reveals a dodecameric structure reminiscent of a barrel with a large channel at its center that appears to contain a closed periplasmic gate. The GspD periplasmic domain forms a vestibule with a conserved constriction, and binds to a pentameric exoprotein and to the trimeric tip of the T2SS pseudopilus. By combining our results with structures of the cholera toxin and T2SS pseudopilus, we provide a structural basis for a possible secretion mechanism of the T2SS.

Keywords

secretin; GspD; electron cryomicroscopy (cryoEM); type II secretion system (T2SS); XcpQ

One or more variants of the type II secretion system (T2SS) occur in many proteobacteria including several important pathogens of humans and plants[1]. One such pathogenic bacterium is *Vibrio cholerae* which uses its T2SS to secrete, amongst other proteins, the major virulence factor cholera toxin (CT) in a folded state from the periplasm across the outer membrane[2,3]. Heat-labile enterotoxin (LT), produced by enterotoxigenic *Escherichia coli* (ETEC) is related to CT in sequence and structure, and is also secreted by a T2SS[4,5]. Both CT and LT are heterohexamers composed of one A and 5 B subunits (AB_5). Although the secretion signals of proteins secreted by the T2SS are still unknown, in the case of both the CT and LT toxins the secretion signal resides in the B-pentamer and not in the A-subunit[6,7]. Due to the apparent lack of a linear secretion signal sequence it has been

$ To whom correspondence should be addressed T.G. (tgonen@u.washington.edu) or W.G.J.H. (wghol@u.washington.edu).

[3]These authors contributed equally to this work

Accession codes: The density map of *Vc*GspD has been deposited at the EM Database accession number EMD-1763.

Author contributions: TG and WGJH designed the research. KVK cloned, expressed, purified protein samples, constructed the molecular models of the periplasmic rings of *Vc*GspD and of the pseudopilus, and performed SPR experiments. SLR collected and processed the cryomicroscopy data and prepared all figures. All authors wrote the manuscript.

suggested that the secretion signal is instead a structural motif present in the native or near-native protein structure[8-11].

The T2SS is a multi-protein macromolecular machine that spans both the inner and outer membrane of the bacteria[12,13]. On its cytosolic side, the T2SS contains a secretion ATPase called GspE that is associated with an inner membrane platform comprising multiple copies of the proteins GspL, GspM, GspF and GspC. A second T2SS sub-assembly is the so-called pseudopilus consisting of the pseudopilins GspG, GspH, GspI, GspJ and GspK. The pseudopilus is thought to act as a plug and/or piston during the secretion of proteins and of toxins[14-16].

The major outer membrane protein of the T2SS is the “secretin” GspD, which forms one of the largest multimeric assemblies in the outer membrane of bacteria. In *Pseudomonas* species, GspD is also called XcpQ; in *Vibrio* species EpsD. The secretins form a diverse family of proteins, occurring in a wide variety of bacteria, with a complex and variable multi-domain structure. Homologues of the T2SS-related secretins are critically important components of other macromolecular assemblies such as the type III secretion system (T3SS), the type IV pilus biogenesis system (T4PBS) and the filamentous phage assembly system[17-26]. These systems occur in a wide variety of bacteria and perform a large number of sophisticated functions, including bacteriophage extrusion, pilus extension and retraction, twitching motility, DNA uptake, injection of proteins directly into target cells, and secretion of proteins into the extracellular milieu.

Here we used electron cryomicroscopy (cryoEM) and single particle reconstruction to determine the 19 Å resolution structure of the T2SS secretin GspD from *V. cholerae* (*Vc*GspD). Previous secretin reconstructions determined by cryoelectron microscopy have been reported with comparable resolutions[23,21], however the *Vc*GspD reconstruction reported here is structurally the most complete representation of a T2SS secretin to date. The *V. cholerae* secretin appears as a 200 Å tall dodecameric channel with a largely unobstructed periplasmic vestibule that contains a constriction site and is separated by a gate from an extracellular chamber that is connected to the extracellular milieu by a cap. Crystal structures of periplasmic GspD subdomains fit well within the contoured features of the cryoEM map. This conserved periplasmic domain is shown to bind to a T2SS exoprotein and also to the pseudopilus tip complex. By combining our results with structural data on a large exoprotein, the ∼85 kDa cholera toxin, and our recent crystal structure of the tip of the pseudopilus of the T2SS, we provide a structural basis for a possible secretion mechanism of exoproteins by the T2SS in which the secretin constriction site plays a critical role.

Results

Electron cryomicroscopy of recombinant *V. cholerae* GspD

Full-length *Vc*GspD was over-expressed in *E. coli*. Intact channels were isolated from the membrane fraction and purified to homogeneity (Fig. 1a and b). The suitability of the preparation for analysis under cryogenic conditions was initially assayed by negative stain electron microscopy (data not shown). Purified *Vc*GspD was prepared for cryomicroscopy using a vitrification robot (Vitrobot, FEI) and continuous carbon copper grids rather then

holey carbon grids to circumvent particle orientation difficulties in ice (Fig. 1c). Approximately 20,000 vitrified *Vc*GspD particles were initially selected in Ximdisp[27] from electron micrographs and classified using reference-free computational alignment routines in SPIDER (Fig. 1c, *inset*)[28].

In side views, the *Vc*GspD particles appear as striated elongated structures (indicated by arrow-heads in Fig. 1c and *inset bottom panel*). A strong band of density bisects the center of the *Vc*GspD particle, and appears to separate the periplasmic and the extracellular domains of the channel. When viewed axially, along the channel pore axis, the *Vc*GspD appears as a ring of density with weak radial densities, or "spokes" (Fig. 1c, *inset top panel*). These radial spokes were used to assign the rotational symmetry to *Vc*GspD channels using real-space symmetry averaging and rotational power spectra analysis[29] (Supplementary Fig. 1). This analysis strongly suggests that *Vc*GspD is a dodecamer and is in agreement with mass estimates by size exclusion chromatography.

The three-dimensional (3D) reconstruction of *Vc*GspD was performed in FREALIGN[30] using the best ∼10,000 particles with an applied 12-fold rotational symmetry. The resulting density is ∼19 Å in resolution as determined by the 0.5 Fourier shell correlation (FSC) criteria (Supplementary Fig. 2). Two-dimensional back-projections of the *Vc*GspD cryoEM map demonstrated a very good fit to the raw image data (data not shown). The density map was contoured at 3.4σ above noise, yielding a ∼0.9 MDa molecular mass consistent with 12 subunits of *Vc*GspD per particle.

Architecture of the *Vc*GspD secretin channel

The *Vc*GspD cryoEM density reveals a cylindrical channel assembly, ∼155 Å in diameter, ∼200 Å in length and a girdled waist (Fig. 2). In side view, the periplasmic domain of the channel is at the bottom followed by an outer membrane domain, and an extracellular domain that is at the very top. The surface of the outer membrane domain appears smooth (possibly due to detergent and/or lipid molecules surrounding the transmembrane domain of the channel) while the surface of the periplasmic domain appears highly contoured and segmented with clear 12-fold symmetric features. The 12-fold radial spoke densities observed in projection averages are found radiating off the bottom of the periplasmic domain when the map is displayed at a slightly lower contour level (Fig. 1c, *inset* compared with Fig. 2c and Supplementary Fig. 1). These spoke features radiating off the periplasmic domain likely correspond to the disordered N-terminal signaling sequence that is retained by *Vc*GspD in our *E. coli* expression system (see Methods section). Projection views of the *Vc*GspD reconstruction reveal additional 12-fold symmetric features that can be observed throughout the architecture of the channel (Supplementary Fig. 1).

Additional features become apparent in a cross section through the *Vc*GspD channel (Fig. 2d). The periplasmic domain of the channel accounts for ∼125 Å out of the total 200 Å length of the channel. The opening to the periplasmic vestibule is ∼75 Å in diameter while its walls are ∼40 Å thick. Approximately two-thirds of the way into the periplasmic vestibule a constriction is identified that narrows the channel's internal diameter to ∼55 Å. A continuous density, which we refer to as the periplasmic gate, seals off the periplasmic vestibule from the extracellular chamber of the channel.

The outer membrane and the extracellular domains of *Vc*GspD account for 75 Å out of the total 200 Å length of the channel. Immediately following the periplasmic gate, the extracellular domain of *Vc*GspD appears as a chamber ∼100 Å in diameter (Fig. 2d). A puckered density that forms a second gate structure caps the top of this chamber. We refer to this second gate as the extracellular gate. In sharp contrast with the periplasmic gate that appears as a solid density, the extracellular gate seems to leave a small opening of ∼10 Å in diameter suggesting that this gate does not form a tight seal across the channel pore. The walls surrounding the extracellular chamber are ∼20 Å thick and appear smooth, possibly due to the presence of detergent and/or lipid molecules as discussed above, but also consistent with the predicted β-barrel topology for this domain of *Vc*GspD and related secretins[18].

Global aspects of our *Vc*GspD architecture agree with the cryomicroscopy reconstruction[23] of the T2SS secretin from *Klebsiella oxytoca* (*Ko*GspD), also called PulD. The non-trypsinized *Ko*GspD multimer was also a 12-fold symmetric channel with outer and inner diameters as observed in the *Vc*GspD structure. However, the membrane-spanning segment of *Ko*GspD was relatively poorly defined and the periplasmic vestibule of *Vc*GspD is ∼80 Å longer than in the *Ko*GspD study (Supplementary Fig. 3). This additional density has allowed us to place the recently determined crystal structures of the N-terminal subdomains of *Ec*GspD[31] into the *Vc*GspD electron microscopy reconstruction as discussed below. The entrance to the periplasmic vestibule in the *Ko*GspD reconstruction was ∼55 Å wide which we can now attribute to the constriction site in our more complete reconstruction. The extracellular gate in our *Vc*GspD reconstruction is a novel feature that has not been previously observed in reported secretin reconstructions. We propose a critical role for this domain in the secretion mechanism of the T2SS as the final channel gate that allows exoprotein release into the extracellular environment (see Discussion).

The secretin architecture in diverse secretion systems

Members of the bacterial outer membrane secretin family are found in the T2SS, the T3SS, the T4PBS, and the filamentous phage secretion systems[17],[18]. Amino acid sequence analysis was used to compare the domain organization of secretins from these four secretion systems (Fig. 3a and Supplementary Fig. 4). All members of the secretin family contain a defining large C-terminal core domain, called the “secretin domain” (Pfam family PF00263[32], cyan in Fig. 3a and Supplementary Fig. 4). Variable regions, that are secretion system and species-specific, flank this defining core domain. The N-terminal region of members of the secretin family is modular and all of these secretins minimally contain (i) the N-terminal N0-like and (ii) the N3-like subdomains directly preceding the C-terminal defining secretin domain (Fig. 3a). These sequence-based analyses indicate a both considerable similarity and substantial differences in domain organization of secretins in the outer membrane of many bacterial secretion/biogenesis systems including the secretins from the T2SS, T3SS, T4BPS and the filamentous phage assembly system.

The domain architecture of secretins from the T2SS and T3SS appear most similar among these four systems, both containing N-terminal modules named the N0, N1 and N3 subdomains (Fig. 3a and Supplementary Fig. 4). The N0 subdomains of the T2SS and T3SS

assume the same topology despite low amino acid sequence identity, with a fold related to the signaling domain of TonB-dependent receptors and bacteriophage tail proteins[31,33]. The structures of the T2SS N1 and N2 subdomains have the same KH domain fold and it has been predicted that the T2SS N3 subdomain has the same structure, which is also shared with the T3SS N1 and N3 subdomains (Supplementary Figs. 4 & 5). Interestingly, T3SS secretins lack the N2 subdomain that is found in the T2SS secretins.

Secretins from the T3SS have been studied by single particle electron microscopy as part of the assembled T3SS complex, in both its closed and open states (Fig. 3b)[24-26]. Like the T2SS, the T3SS is a large multi-protein complex that spans both the inner and outer membrane of bacteria. The T3SS base complex mainly consists of the outer membrane secretin, sitting on top of a T3SS inner membrane complex (Fig. 3b, center). The cryoEM reconstruction of the T2SS *Vc*GspD secretin resembles that of the T3SS secretin in the closed state without needle (Fig. 3b, left compared with center). In both structures the large periplasmic gate appears closed and the ~55 Å wide periplasmic constriction is apparent, approximately equally distant from the periplasmic gate. The reconstructions of the fully assembled T3SS [24,26] noticeably lack the extracellular gate observed in the *Vc*GspD secretin. This feature may therefore be specific to the T2SS secretins, however, it is also possible that this domain was not resolved in the available T3SS reconstructions. Further structural studies will be required to dissect these structural differences.

The outer membrane pore-forming channel from the type IVa secretion system (T4aSS) has been recently characterized by X-ray crystallography[34] and as part of the assembled T4aSS by cryoEM[35]. The T4aSS outer membrane channels do not appear genetically related to the secretin family of outermembrane channels[34] (and indeed appear overall structurally unique, and also different from the type IVb secretion system[36-38]) nevertheless a side-by-side structural comparison does reveals some common global structural outside shape features), yet, the internal shape is distinctly different (compare e.g. Fig. 3b with Fig. 4c from [ref. 34]; Supplementary Fig. 6).

Molecular modeling of GspD N0-N3 and substrate interaction

The periplasmic domain of *Vc*GspD density is modular. In cross-section, the walls of this domain that form the periplasmic vestibule of the channel appear as concentric rings of density (Fig. 2d). Indeed the periplasmic N-terminus of secretins from the T2SS contains four periplasmic subdomains N0-N3 (Fig. 3a and Fig. 4). We recently published the crystal structure of the N-terminal periplasmic subdomains N0-N1-N2 from the homologous ETEC GspD secretin[31]. The crystal structure revealed a modular architecture, composed of 3 consecutively linked domains with mixed α/β topology. The modular features resolved within the periplasmic domain of the *Vc*GspD cryoEM map correspond well with the modular architecture observed in the crystal structures of periplasmic *Ec*GspD. Although our crystal structure did not include N3, this domain is related in sequence to both N1 and N2 with strong predicted structural homology ([31]; Pfam family PF03958[32]).

Since the sequence similarity between *Ec*GspD and *Vc*GspD is very high, with 54% amino acid sequence identity for these subdomains (Supplementary Fig. 4), we used the crystal structure of periplasmic *Ec*GspD to fit the N0-N1-N2-N3 subdomains. We first used the

program SymmDock[39] to generate 12-fold symmetrical rings (Fig. 4a). The N0 and N1 domains were treated as a single complex, as observed in the crystal structure of periplasmic *Ec*GspD, whereas the N2 and N3 ring models were treated independently, since these are tethered by flexible linkers (Supplementary Fig. 4).

The fitted periplasmic ring models match well within the modular contours of the *Vc*GspD cryoEM map (Fig. 4 **and** Supplementary Fig. 7). The N0-N1 ring fitted into the ∼40 Å lobe of density at the very bottom of the *Vc*GspD periplasmic vestibule. The N2 and N3 rings fitted well directly above the N0-N1 ring (Fig. 4a). This arrangement matched the contours of the periplasmic domain, placing the N2 subdomain into the central segment of this region, and positioning the N3 subdomain snuggly into the volume encompassing the periplasmic constriction. The fit of the N3 subdomain at the periplasmic constriction is consistent with proteolysis studies of *Ko*GspD[23] (Supplementary Fig. 3).

To investigate the possible functional role of the GspD periplasmic domain, we characterized by surface plasmon resonance (SPR) the interactions between: (i) the periplasmic domain of the secretin from enterotoxigenic *E. coli* (specifically the fragment containing *Ec*GspD subdomains N0-N1-N2[31], (ii) the B-pentamer of heat-labile enterotoxin (LT-B_5) which is secreted by the T2SS of enterotoxigenic *E. coli*[5] and (iii) the trimeric complex *Ec*GspK-GspI-GspJ[40] that forms the tip of the T2SS pseudopilus (Fig. 4b). Our analysis showed that the secretin *Ec*GspD binds independently to exoprotein LT and to the pseudopilus tip complex. In contrast, we did not detect binding between LT and the pseudopilus tip complex (data not shown), which may reflect either a lack of interaction or a requirement for additional T2SS proteins. Together, these data suggest that the secretin periplasmic domain has an important functional role in recognition of both the exoprotein and the secretion machinery.

The N3 periplasmic domain fits into the constriction of the *Vc*GspD density (Fig. 4a). The N3 periplasmic domain appears to be highly conserved at the amino acid level, even in distantly related secretins (Fig. 3a and Supplementary Fig. 4) suggesting that this domain plays a conserved mechanistic role in these secretion systems. Such a role is supported by a recent study that identified several amino acids within the N3 domain of the secretin pIV from the filamentous phage assembly system that resulted in a “leaky” channel phenotype when mutated[41]. To gain further insight into the mechanistic role of this conserved domain, we placed the structure of the cholera toxin (CT) heterohexamer AB_5[42] into the *Vc*GspD secretin density (Fig. 4c). Our analysis shows that the periplasmic vestibule of the secretin channel is large enough to accommodate the CT although it is a snug fit. The ∼65 Å wide CT structure fits well within the ∼75 Å wide vestibule created by the N0-N2 domains without any obvious steric hindrance. In sharp contrast, the CT will not be able to fit through the constriction formed by N3 (∼55 Å diameter) without inducing a major conformational change in the secretin. The N3 subdomain may therefore be important for T2SS exoprotein recognition and secretion at least for larger exoproteins like the ∼85 kDa cholera toxin and heat-labile enterotoxin (LT). For smaller exoproteins, like e.g. the ∼36 kDa pectate lyase from *Dickeya dadantii* (*Erwinia chrysanthemi*)[43], there might be a different process in operation since such small proteins would not be blocked by the T2SS constriction. It is of interest that the diameter of the GspK-GspI-GspJ tip of the pseudopilus is ∼54 Å[40], i.e.

essentially the same as the cross-section of the *Vc*GspD constriction. Therefore in such cases the tip of the pseudopilus might be interacting with the constriction and cause conformational changes leading to opening of the gate in the T2SS secretin channel.

Discussion

The mechanism of protein secretion by the T2SS is essentially unknown. The T2SS contains a pseudopilus, which has been suggested to act either as a plug to close the outer membrane pore or as a piston involved in pushing toxins and other secreted proteins through the secretin pore[14-16]. Our electron cryomicroscopy reconstruction of the secretin *Vc*GspD clearly identifies a periplasmic gate and the channel appears to be in its closed state (Figs. 2, 3 **and** 4). Since the channel is already closed it seems likely that the function of the pseudopilus in secretion would be to act as a piston to push exoproteins out, yet, at the same time may serve as a plug to seal the pore once the periplasmic channel gate is opened.

The crystal structures of all pseudopilins have been recently determined including the ternary complex of the GspK-GspI-GspJ at the very tip of the pseudopilus[40,44-47]. In the following paragraphs, we combine this wealth of recent structural information with our new electron cryomicroscopy structure of the secretin to show how the piston mechanism for toxin secretion by the T2SS could work, with the secretin constriction playing a key role (Fig. 5).

The piston secretion model could start with the tip of the pseudopilus interacting with cholera toxin and aligning its helix axis with the pore axis of the secretin. It is also possible that the toxin, and other exoproteins in general, may be recruited initially into the secretin periplasmic vestibule followed by a second step in which the growing pseudopilus translocates the exoprotein through the secretion machinery[14] (Fig. 5, left). Our binding data (Fig. 4b) indicate that exoproteins are recruited directly by the secretin by binding to the periplasmic domain of the channel (illustrated in Fig. 5, left). At this stage, the secretin itself is in its closed state. Next, the pseudopilus begins to polymerize and extend, pushing the toxin into the periplasmic vestibule of the secretin (Fig. 5, middle). The periplasmic vestibule of the secretin is wide enough to accommodate the toxin and the pseudopilus. Once the toxin or the tip of the pseudopilus reaches the N3 domain of the secretin (the constriction) the channel will need to undergo a conformational change to open the pore and allow the toxin to be secreted (Fig. 5, right). This conformational change may resemble the conformational change that was observed in the T3SS upon needle attachment (Fig. 3b, middle panel compared with right panel; see also[26]). Namely, the secretin N3 constriction would move outward, expanding the constriction from ∼55 Å to a larger diameter of ∼70-90 Å to let the toxin and pseudopilus pass. At the same time, the periplasmic gate would open and the toxin could then enter the extracellular chamber of the secretin (Fig. 5, right). No pseudopilus component of the T2SS has ever been observed outside the cell under physiological conditions[48-50]. It is therefore likely that the tip of the pseudopilus never passes the periplasmic gate of the secretin, and is used as a piston to push exoproteins into the periplasmic chamber of the secretin channel, possibly also to induce a conformational change in the secretin by interactions with the N3 constriction. Upon opening of the periplasmic gate, the pseudopilus may move the exoprotein through the opened gate and at

the same time remain extended serving as a plug to prevent channel leakage. Once the exoprotein is loaded into the extracellular chamber, the extracellular gate opens and the exoprotein can be released. After the exoprotein is released, the extracellular and periplasmic gates are likely to close, and the pseudopilus would no longer be required as a plug.

Our structures support a piston driven secretion mechanism with a critical role for the constriction site in the periplasmic vestibule of GspD. This model is in line with current structural and biochemical studies. However, we must note, that whereas secretin interaction with the exoprotein has been reported before[14] and is also shown here, it is still not known whether *(i)* the pilus directly interacts with exoproteins with the aid of additional T2SS proteins or (yet-to-be-identified) adapters; and, *(ii)* other T2SS proteins, such as GspC[51,52], may play a key role in inducing conformational changes of the secretin. Future studies must be carried out to answer these questions regarding the intriguing T2SS.

Methods

Expression and purification of recombinant *Vc*GspD channels

The full-length gene of *V. cholerae* GspD (*Vc*GspD) was cloned into pET-22b(+) vector from pMMB710 plasmid (a generous gift from Michael Bagdasarian, Michigan State University) to encode a C-terminal hexahistidine tag. *Vc*GspD was expressed in Tuner(DE3)pLacI strain by growing the cells to A_{600}=0.8 and induced with 0.1 mM IPTG. Cells were harvested 3 h post-induction, resuspended in 20 mM Tris-HCl pH 7.8, 300 mM NaCl and disrupted using a French press. The membrane fraction was isolated by ultracentrifugation and membrane proteins were solubilized using N-dodecyl-N,N′-dimethylammonio-1-propanesulfonate (SB3-12). *Vc*GspD was purified using Ni-affinity and size-exclusion chromatography (Fig. 1a and b). The N-terminal sequencing results (not shown) indicated that the signal peptide was intact. This also occurs upon replacement of the native signal *Vc*GspD sequence with *pelB* signal sequence. Those results suggest that *Vc*GspD is targeted to the inner membrane in our expression system, similar to *Ko*GspD in the absence of a cognate pilotin protein GspS[53]. It should be noted that no pilotin homologs have been identified so far in the *V. cholerae* genome.

Electron cryomicroscopy and image processing

*Vc*GspD was prepared for electron cryomicroscopy by applying a 2 μl drop of sample (~0.05 mg ml^{-1}) to a negatively charged Quantifoil holey carbon specimen grid (Quantifoil, Germany) overlayed with a continuous layer of carbon. The sample was blotted with filter paper and plunged into liquid ethane using a Vitrobot (FEI, Hilsboro, Oregon). The frozen specimen was loaded to a Gatan cryo holder and inserted into a FEI Tecnai F20 microscope, equipped with a field emission gun operated at 200 kV under low dose conditions. Images were recorded on film (Kodak SO-163) at a magnification of 50,000× and defocus values ranging from 1.5 to 5.0 μm. The film was digitized with a 6.9 μm step size, and binned twice, yielding a final pixel size of 2.54 Å per pixel. Thon rings in the power spectra were used to select only those micrographs free of drift or significant astigmatism. The contrast transfer function (CTF) parameters were determined for each micrograph using the program

CTFTILT[54]. Approximately 20,000 particles were selected using Ximdisp[27] and processed in SPIDER[28] for generating multivariate reference free class averages. Rotational symmetry of *Vc*GspD was determined from axially oriented particles, using real space symmetry averaging in EMAN[55] and rotational power spectra analysis using RotaStat[29] (Supplementary Fig. 1).

Three-dimensional reconstruction and refinement of *Vc*GspD

A low-resolution density map of *Vc*GspD was initially obtained from negatively stained particles in SPIDER[28] and used as an initial search model for our best 10,000 particle images in FREALIGN ver. 7[30]. Search and refine protocols were used in FREALIGN to determine initial Euler angles and x, y shifts relative to the initial search model for each particle and then refined with an applied C12 rotational symmetry through consecutive rounds of parameter refinement and three-dimensional reconstruction until no improvement in alignment parameters were observed. The nominal resolution of the final reconstruction was estimated from where the Fourier shell correlation (FSC) curve fell to a value of 0.5[56], corresponding to 19 Å (Supplementary Fig. 2). The final map was filtered to 19 Å and normalized using MAPMAN[57]. The map was visualized and prepared for figures using UCSF Chimera[58] at a contour level of 3.4σ, corresponding to an approximate 0.9 MDa volume[59]. Figure 2c was prepared using a 2.4σ contour level to show the “spoke” features observed in projection averages. Our C12 symmetry assignment of *Vc*GspD was supported by comparing the results obtained when alternative symmetries were applied to the reconstruction (Supplementary Fig. 1).

Creation of periplasmic *Vc*GspD rings, cholera toxin and pseudopilus models

The modeling of C12 symmetry periplasmic *Vc*GspD rings was performed using the program SymmDock[39] using methods previously described[47]. A model of the pseudopilus was used based on the helical parameters from the GspK-GspI-GspJ complex, by adding additional pseudopilins to the tip[40]. A molecular model for the export of a secreted protein by the T2SS was then obtained by aligning the helical axis of the pseudopilus with the 12-fold symmetry axis of the GspD reconstruction, and placing the structure of cholera toxin[42] on top of the GspK-GspI-GspJ tip with the 5-fold axis of symmetry coinciding with the 12-fold and helical axes(Fig. 5).

Fitting of models into *Vc*GspD reconstruction

Periplasmic *Vc*GspD ring models were fit into the density map of *Vc*GspD as follows. The 10 lowest energy ring models for each the N0/1, N2 and N3 domains calculated by SymmDock were initially placed into the density map of *Vc*GspD (Supplementary Fig. 7). The N0/N1 domain was treated as a single complex and the ring models for this domain was placed at the very bottom of the periplasmic domain of the *Vc*GspD map, with the N-terminus pointed downward (toward the periplasm). The N2 and N3 ring models were treated separately as tethered by flexible linkers and placed in an N- to C-terminal (head-to-tail) fashion. These initial placements were optimized by automated fitting procedures in UCSF Chimera[58]. The ring models for each domain with the best correlation to the

experimental map were selected. The final N0-N3 periplasmic domain model gave a cross-correlation score of 0.65 compared the experimental map (Supplementary Fig. 7).

Surface plasmon resonance studies

The B-pentamer of heat-labile enterotoxin (LTB_5), the *Ec*GspD fragment 1-237 (peri-GspD) corresponding to the N0-N1-N2 subdomains, and the trimeric pseudopilus tip complex *Ec*GspK-GspI-GspJ were each expressed and purified as described[31,40,60]. peri-GspD was immobilized on a CM5 research-grade sensor chip (GE Healthcare) by amine coupling chemistry using the manufacturer's protocols and LTB_5 and *Ec*GspK-GspI-GspJ were used as the analyte. SPR measurements were carried out in HBS-EP buffer (10 mM HEPES pH 7.4, 150 mM NaCl, 3 mM EDTA, 0.005% P-20 surfactant) at 25° C using Biacore T100 system (GE Healthcare). The interaction of LTB_5 with peri-GspD was confirmed using an immobilized LTB_5 and peri-GspD as analyte; however, in this case no steady state binding was observed due to homophilic GspD interactions (data not shown). Data were analyzed with Biacore T100 Evaluation software, ver. 2.0.1.

Supplementary Material

Refer to Web version on PubMed Central for supplementary material.

Acknowledgments

We thank the Murdock Charitable Trust and the Washington Research Foundation for generous support of our electron cryomicroscopy facility. We are grateful to Ji Sun, Melissa Gonen, Breanna Vollmar, and Stewart Turley for contributions to the earlier stages of this work; Michael Bagdasarian for a *Vc*GspD-containing plasmid; and Jaclyn DelaRosa for assistance with protein preparation. We thank Alexey J. Merz (University of Washington) for helpful discussions. We thank Natalia Korotkova and Paul Wallace for discussion of SPR experiments. Part of this work was conducted at the University of Washington NanoTech User Facility, a member of the NSF National Nanotechnology Infrastructure Network (NNIN). This research is supported by the National Institutes of Health grant AI34501. TG is a Howard Hughes Medical Institute Early Career Scientist. The authors declare that none have a financial interest related to this work.

References

1. Cianciotto NP. Type II secretion: a protein secretion system for all seasons. Trends Microbiol. 2005; 13:581–588. [PubMed: 16216510]
2. Hirst TR, Sanchez J, Kaper JB, Hardy SJ, Holmgren J. Mechanism of toxin secretion by *Vibrio cholerae* investigated in strains harboring plasmids that encode heat-labile enterotoxins of *Escherichia coli*. Proc Natl Acad Sci U S A. 1984; 81:7752–6. [PubMed: 6393126]
3. Streatfield SJ, et al. Intermolecular interactions between the A and B subunits of heat-labile enterotoxin from *Escherichia coli* promote holotoxin assembly and stability in vivo. Proc Natl Acad Sci U S A. 1992; 89:12140–4. [PubMed: 1465452]
4. Sixma TK, et al. Crystal structure of a cholera toxin-related heat-labile enterotoxin from *E. coli*. Nature. 1991; 351:371–377. [PubMed: 2034287]
5. Tauschek M, Gorrell RJ, Strugnell RA, Robins-Browne RM. Identification of a protein secretory pathway for the secretion of heat-labile enterotoxin by an enterotoxigenic strain of *Escherichia coli*. Proc Natl Acad Sci U S A. 2002; 99:7066–71. [PubMed: 12011463]
6. Hirst TR, Holmgren J. Conformation of protein secreted across bacterial outer membranes: a study of enterotoxin translocation from *Vibrio cholerae*. Proc Natl Acad Sci U S A. 1987; 84:7418–22. [PubMed: 3478701]

7. Leece R, Hirst TR. Expression of the B subunit of Escherichia coli heat-labile enterotoxin in a marine Vibrio and in a mutant that is pleiotropically defective in the secretion of extracellular proteins. J Gen Microbiol. 1992; 138:719–24. [PubMed: 1588306]
8. Chapon V, Simpson HD, Morelli X, Brun E, Barras F. Alteration of a single tryptophan residue of the cellulose-binding domain blocks secretion of the Erwinia chrysanthemi Cel5 cellulase (ex-EGZ) via the type II system. J Mol Biol. 2000; 303:117–23. [PubMed: 11023779]
9. Francetic O, Pugsley AP. Towards the identification of type II secretion signals in a nonacylated variant of pullulanase from Klebsiella oxytoca. J Bacteriol. 2005; 187:7045–55. [PubMed: 16199575]
10. Voulhoux R, Taupiac MP, Czjzek M, Beaumelle B, Filloux A. Influence of deletions within domain II of exotoxin A on its extracellular secretion from Pseudomonas aeruginosa. J Bacteriol. 2000; 182:4051–8. [PubMed: 10869085]
11. Braun P, Tommassen J, Filloux A. Role of the propeptide in folding and secretion of elastase of Pseudomonas aeruginosa. Mol Microbiol. 1996; 19:297–306. [PubMed: 8825775]
12. Johnson TL, Abendroth J, Hol WG, Sandkvist M. Type II secretion: from structure to function. FEMS Microbiol Lett. 2006; 255:175–186. [PubMed: 16448494]
13. Michel, GPF.; Voulhoux, R. The Type II Secretory System (T2SS) in Gram-negative Bacteria: A Molecular Nanomachine for Secretion of Sec and Tat-Dependent Extracellular Proteins. In: Wooldridge, K., editor. Bacterial Secreted Proteins: Secretory Mechanisms and Role in Pathogenesis. Caister Academic Press; 2009. p. 67-92.
14. Shevchik VE, Robert-Baudouy J, Condemine G. Specific interaction between OutD, an Erwinia chrysanthemi outer membrane protein of the general secretory pathway, and secreted proteins. EMBO J. 1997; 16:3007–3016. [PubMed: 9214618]
15. Filloux A, Michel G, Bally M. GSP-dependent protein secretion in gram-negative bacteria: the Xcp system of *Pseudomonas aeruginosa*. FEMS Microbiol Rev. 1998; 22:177–98. [PubMed: 9818381]
16. Sandkvist M. Biology of type II secretion. Molecular Microbiology. 2001; 40:271–283. [PubMed: 11309111]
17. Martin PR, Hobbs M, Free PD, Jeske Y, Mattick JS. Characterization of pilQ, a new gene required for the biogenesis of type 4 fimbriae in Pseudomonas aeruginosa. Mol Microbiol. 1993; 9:857–868. [PubMed: 7901733]
18. Genin S, Boucher CA. A superfamily of proteins involved in different secretion pathways in gram-negative bacteria: modular structure and specificity of the N-terminal domain. Mol Gen Genet. 1994; 243:112–118. [PubMed: 8190064]
19. Brok R, et al. The C-terminal domain of the Pseudomonas secretin XcpQ forms oligomeric rings with pore activity. J Mol Biol. 1999; 294:1169–1179. [PubMed: 10600375]
20. Collins RF, Davidsen L, Derrick JP, Ford RC, Tonjum T. Analysis of the PilQ secretin from Neisseria meningitidis by transmission electron microscopy reveals a dodecameric quaternary structure. J Bacteriol. 2001; 183:3825–32. [PubMed: 11395444]
21. Opalka N, et al. Structure of the filamentous phage pIV multimer by cryo-electron microscopy. J Mol Biol. 2003; 325:461–70. [PubMed: 12498796]
22. Burghout P, et al. Structure and electrophysiological properties of the YscC secretin from the type III secretion system of Yersinia enterocolitica. J Bacteriol. 2004; 186:4645–54. [PubMed: 15231798]
23. Chami M, et al. Structural insights into the secretin PulD and its trypsin-resistant core. J Biol Chem. 2005; 280:37732–41. [PubMed: 16129681]
24. Hodgkinson JL, et al. Three-dimensional reconstruction of the Shigella T3SS transmembrane regions reveals 12-fold symmetry and novel features throughout. Nat Struct Mol Biol. 2009; 16:477–85. [PubMed: 19396171]
25. Marlovits TC, et al. Assembly of the inner rod determines needle length in the type III secretion injectisome. Nature. 2006; 441:637–40. [PubMed: 16738660]
26. Marlovits TC, et al. Structural insights into the assembly of the type III secretion needle complex. Science. 2004; 306:1040–2. [PubMed: 15528446]
27. Smith JM. Ximdisp--A visualization tool to aid structure determination from electron microscope images. J Struct Biol. 1999; 125:223–8. [PubMed: 10222278]

28. Frank J, et al. SPIDER and WEB: processing and visualization of images in 3D electron microscopy and related fields. J Struct Biol. 1996; 116:190–9. [PubMed: 8742743]
29. Kocsis E, Cerritelli ME, Trus BL, Cheng N, Steven AC. Improved methods for determination of rotational symmetries in macromolecules. Ultramicroscopy. 1995; 60:219–28. [PubMed: 7502382]
30. Grigorieff N. FREALIGN: high-resolution refinement of single particle structures. J Struct Biol. 2007; 157:117–25. [PubMed: 16828314]
31. Korotkov KV, Pardon E, Steyaert J, Hol WG. Crystal structure of the N-terminal domain of the secretin GspD from ETEC determined with the assistance of a nanobody. Structure. 2009; 17:255–65. [PubMed: 19217396]
32. Finn RD, et al. Pfam: clans, web tools and services. Nucleic Acids Res. 2006; 34:D247–51. [PubMed: 16381856]
33. Spreter T, et al. A conserved structural motif mediates formation of the periplasmic rings in the type III secretion system. Nat Struct Mol Biol. 2009; 16:468–76. [PubMed: 19396170]
34. Chandran V, et al. Structure of the outer membrane complex of a type IV secretion system. Nature. 2009; 462:1011–5. [PubMed: 19946264]
35. Fronzes R, et al. Structure of a type IV secretion system core complex. Science. 2009; 323:266–8. [PubMed: 19131631]
36. Christie PJ, Vogel JP. Bacterial type IV secretion: conjugation systems adapted to deliver effector molecules to host cells. Trends Microbiol. 2000; 8:354–60. [PubMed: 10920394]
37. Vincent CD, et al. Identification of the core transmembrane complex of the Legionella Dot/Icm type IV secretion system. Mol Microbiol. 2006; 62:1278–91. [PubMed: 17040490]
38. Ensminger AW, Isberg RR. Legionella pneumophila Dot/Icm translocated substrates: a sum of parts. Curr Opin Microbiol. 2009; 12:67–73. [PubMed: 19157961]
39. Schneidman-Duhovny D, Inbar Y, Nussinov R, Wolfson HJ. PatchDock and SymmDock: servers for rigid and symmetric docking. Nucleic Acids Res. 2005; 33:W363–7. [PubMed: 15980490]
40. Korotkov KV, Hol WG. Structure of the GspK-GspI-GspJ complex from the enterotoxigenic Escherichia coli type 2 secretion system. Nat Struct Mol Biol. 2008; 15:462–8. [PubMed: 18438417]
41. Spagnuolo J, et al. Identification of the gate regions in the primary structure of the secretin pIV. Mol Microbiol. 2010; 76:133–150. [PubMed: 20149106]
42. O'Neal CJ, Amaya EI, Jobling MG, Holmes RK, Hol WG. Crystal structures of an intrinsically active cholera toxin mutant yield insight into the toxin activation mechanism. Biochemistry. 2004; 43:3772–82. [PubMed: 15049684]
43. Creze C, et al. The crystal structure of pectate lyase peli from soft rot pathogen Erwinia chrysanthemi in complex with its substrate. J Biol Chem. 2008; 283:18260–8. [PubMed: 18430740]
44. Köhler R, et al. Structure and assembly of the pseudopilin PulG. Mol Microbiol. 2004; 54:647–64. [PubMed: 15491357]
45. Yanez ME, Korotkov KV, Abendroth J, Hol WG. Structure of the minor pseudopilin EpsH from the Type 2 Secretion system of *Vibrio cholerae*. J Mol Biol. 2008; 37:91–103. [PubMed: 18241884]
46. Yanez ME, Korotkov KV, Abendroth J, Hol WG. The crystal structure of a binary complex of two pseudopilins: EpsI and EpsJ from the type 2 secretion system of Vibrio vulnificus. J Mol Biol. 2008; 375:471–86. [PubMed: 18022192]
47. Korotkov KV, et al. Calcium is essential for the major pseudopilin in the type 2 secretion system. J Biol Chem. 2009; 284:25466–70. [PubMed: 19640838]
48. Durand E, et al. Type II protein secretion in Pseudomonas aeruginosa: the pseudopilus is a multifibrillar and adhesive structure. J Bacteriol. 2003; 185:2749–58. [PubMed: 12700254]
49. Durand E, et al. XcpX controls biogenesis of the Pseudomonas aeruginosa XcpT-containing pseudopilus. J Biol Chem. 2005; 280:31378–89. [PubMed: 16012171]
50. Vignon G, et al. Type IV-like pili formed by the type II secreton: specificity, composition, bundling, polar localization, and surface presentation of peptides. J Bacteriol. 2003; 185:3416–28. [PubMed: 12754241]

51. Bouley J, Condemine G, Shevchik VE. The PDZ domain of OutC and the N-terminal region of OutD determine the secretion specificity of the type II out pathway of Erwinia chrysanthemi. J Mol Biol. 2001; 308:205–219. [PubMed: 11327762]
52. Korotkov K, Krumm BE, Bagdasarian M, Hol WG. Structural and Functional Studies of EpsC, a Crucial Component of the Type 2 Secretion System from *Vibrio cholerae*. J Mol Biol. 2006; 363:311–321. [PubMed: 16978643]
53. Guilvout I, Chami M, Engel A, Pugsley AP, Bayan N. Bacterial outer membrane secretin PulD assembles and inserts into the inner membrane in the absence of its pilotin. Embo J. 2006; 25:5241–9. [PubMed: 17082772]
54. Mindell JA, Grigorieff N. Accurate determination of local defocus and specimen tilt in electron microscopy. J Struct Biol. 2003; 142:334–47. [PubMed: 12781660]
55. Ludtke SJ, Baldwin PR, Chiu W. EMAN: semiautomated software for high-resolution single-particle reconstructions. J Struct Biol. 1999; 128:82–97. [PubMed: 10600563]
56. Stewart PL, Chiu CY, Haley DA, Kong LB, Schlessman JL. Review: resolution issues in single-particle reconstruction. J Struct Biol. 1999; 128:58–64. [PubMed: 10600559]
57. Kleywegt GJ, Jones TA. xdlMAPMAN and xdlDATAMAN - programs for reformatting, analysis and manipulation of biomacromolecular electron-density maps and reflection data sets. Acta Crystallogr D Biol Crystallogr. 1996; 52:826–8. [PubMed: 15299647]
58. Pettersen EF, et al. UCSF Chimera--a visualization system for exploratory research and analysis. J Comput Chem. 2004; 25:1605–12. [PubMed: 15264254]
59. Matthews BW. Solvent content of protein crystals. J Mol Biol. 1968; 33:491–7. [PubMed: 5700707]
60. Mitchell DD, Pickens JC, Korotkov K, Fan E, Hol WG. 3,5-Substituted phenyl galactosides as leads in designing effective cholera toxin antagonists; synthesis and crystallographic studies. Bioorg Med Chem. 2004; 12:907–20. [PubMed: 14980603]

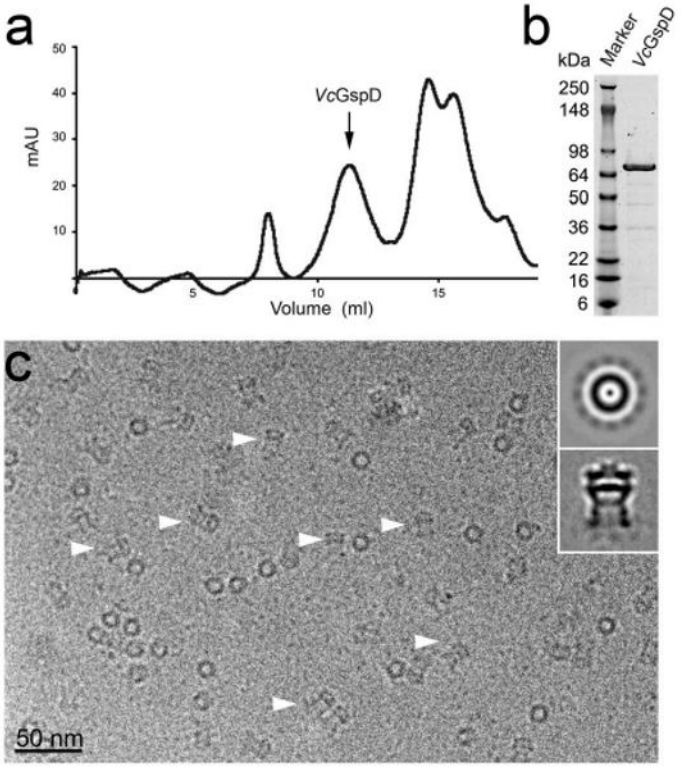

Figure 1. Purification and electron cryomicroscopy of cholera toxin secretion channel *Vc*GspD

(a) *Vc*GspD channels were purified to homogeneity by size-exclusion chromatography. Intact channels eluted as ∼0.9 MDa species (arrow). **(b)** Coomassie blue stained SDS-PAGE of purified *Vc*GspD (∼74 kDa). **(c)** Electron micrograph of vitrified *Vc*GspD channels. (*inset, top panel*) Representative class averages of *Vc*GspD particles. In top views, looking down the channel axis, the particles appear as a ring with a punctate density located at the center of the channel and weaker densities "spokes" surround the channel. Side views (indicated with arrow heads in **(c)**) appear as long striated channels with a strong central density or "plug" that bisects the center of the channel (*inset, bottom panel*).

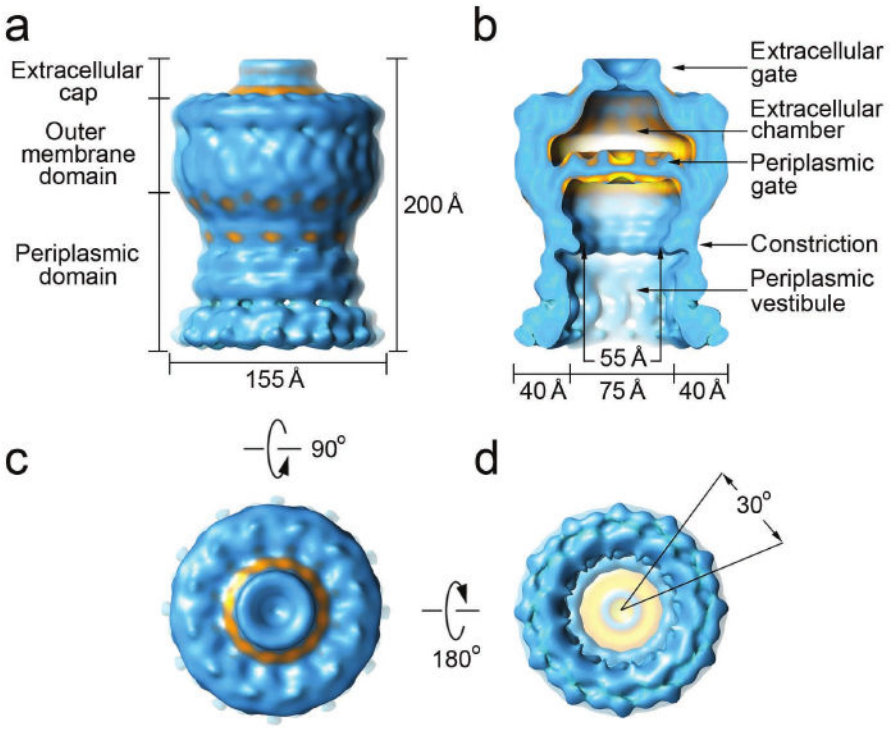

Figure 2. Three-dimensional electron cryomicroscopy reconstruction of *Vc*GspD

(a, c and **d)** Side, top and bottom views, respectively, of the dodecameric *Vc*GspD reconstruction at 19 Å resolution. In side view, three domains are identified from bottom to top as the periplasmic domain, the outer membrane domain and extracellular cap. **(b)** A slice view through the channel reveals the periplasmic vestibule, a constriction, the periplasmic gate, an extracellular chamber and an extracellular gate. The extracellular chamber is ∼100 Å wide whereas the periplasmic vestibule is ∼75 Å in diameter. The periplasmic constriction narrows the vestibule to ∼55 Å.

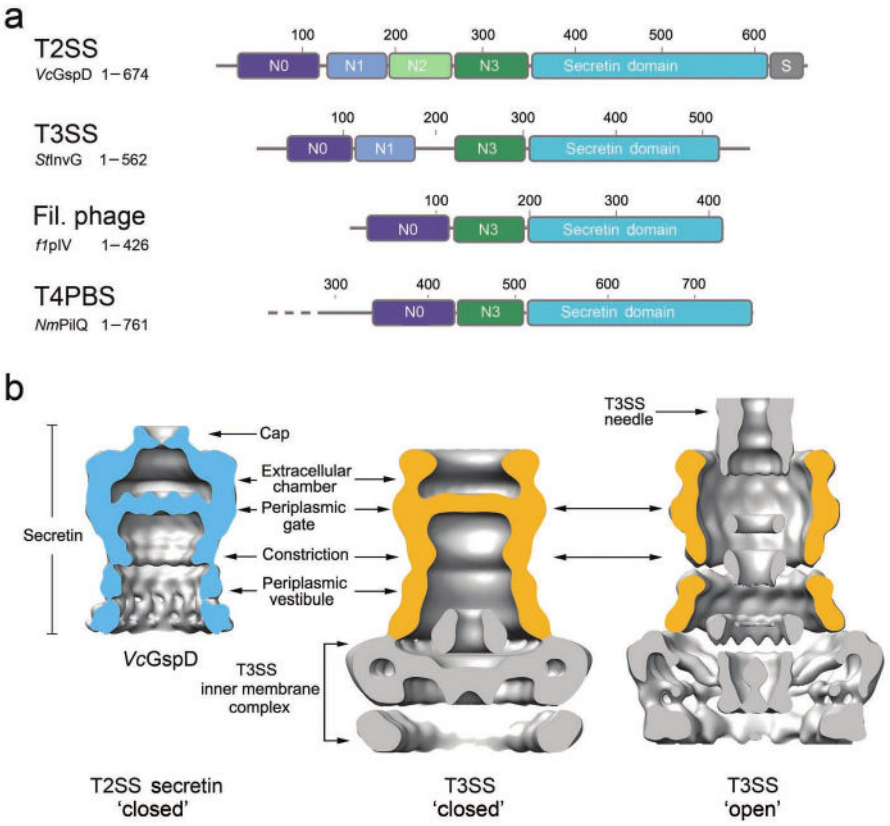

Figure 3. The secretin architecture is conserved in different secretion systems

(a) Domain architecture of secretins from the T2SS, the T3SS, the filamentous phage assembly system and the T4 pilus biogenesis system (T4PBS). Members of the secretin super-family contain a C-terminal secretin core homology domain (cyan)[17,18]. The T2SS secretins generally contain four periplasmic subdomains, termed N0-N3. The N0 subdomain (dark blue) is located at the N-terminus and is followed by the three structurally homologous subdomains, N1-N3 (blue, green and dark green, respectively). A T2SS specific domain, termed the S-domain (grey), is located at the very C-terminus. Secretins from other systems share a similar architecture, composed of the secretin domain and at least two periplasmic subdomains that are structurally equivalent to N0 and N3 of *Vc*GspD. **(b)** Structural comparison of the *Vc*GspD density (blue, *left*) to single particle reconstructions of the T3SS in its close state (*center*) (EMDB 1224[26]) and to the fully assembled T3SS needle complex in its open state (*right*) (EMDB 1617[24]). The outer membrane T3SS secretin sits on top of a large inner membrane complex (gold, *center and right*). *Vc*GspD appears to be in its closed state (*left compared with center*).

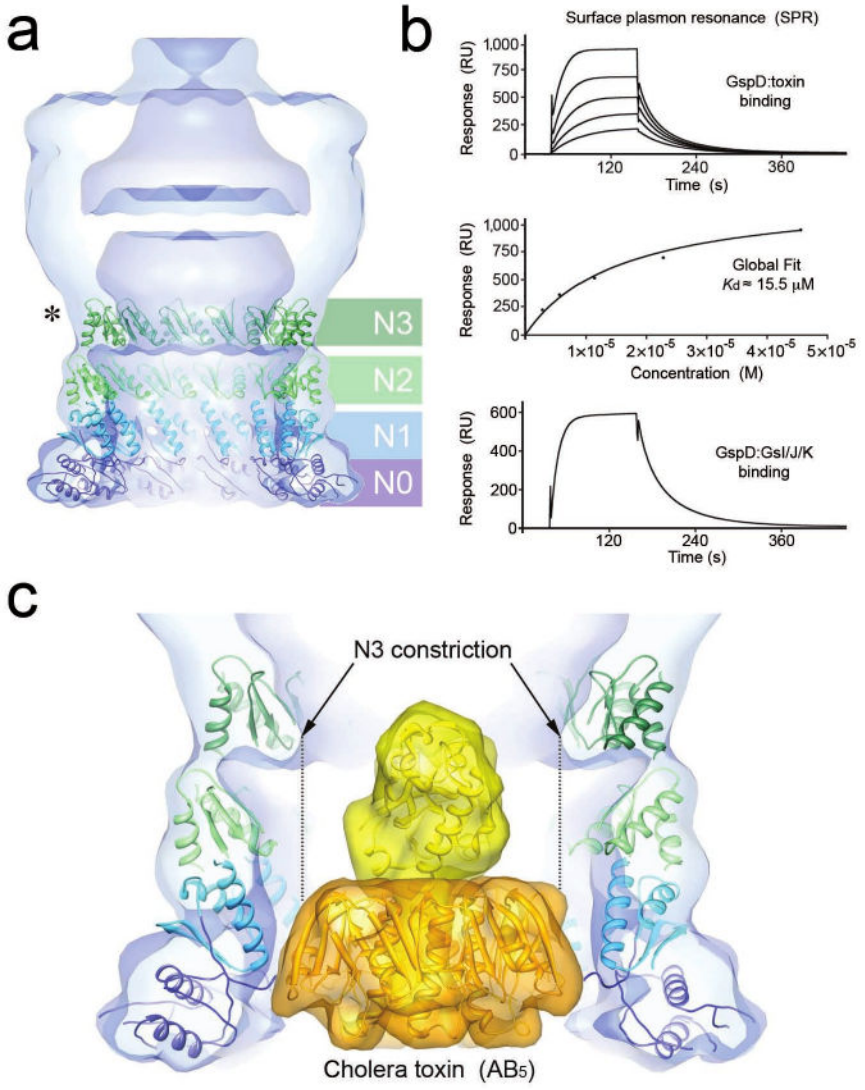

Figure 4. The periplasmic GspD domain contains a conserved N3 constriction and binds to the T2SS exoprotein and pseudopilus tip complex

(a) Fitting of twelve member ring models of the *Vc*GspD N-terminal periplasmic domains (N0-N3) into the *Vc*GspD density map. The N0 domain (dark blue) and N1 domain (light blue) are anchored at the bottom of the *Vc*GspD density map. This places the N2 domain (light green) into the central periplasmic domain density and the N3 domain (dark green) into the periplasmic constriction. This placement correlates well with protease cleavage experiments that cut at N3 (asterisk)[23,33]. **(b)** (*top*) Sensorgram showing binding of the B-pentamer of heat-labile enterotoxin (B_5) to immobilized *Ec*GspD. Relative units (RU, vertical) are plotted as a function of time (in seconds, horizontal). (*middle*) Global fit of equilibrium measurements (RE) depicted above versus B_5 concentrations (M) gives a dissociation constant (*K*d) of ~15.5 μM. (*bottom*) Sensorgram showing the binding of the pseudopilus tip complex *Ec*GspK-GspI-GspJ to immobilized *Ec*GspD. **(c)** Fitting of the cholera toxin AB_5 heterohexamer ([42], PDB ID 1S5E) (A subunit yellow; B subunits gold) into the *Vc*GspD periplasmic vestibule. The ~65 Å wide cholera toxin molecule fits well

within the ~75 Å vestibule formed by the N0-N2 domains but would not fit though the ~55 Å wide constriction composed of the N3 domain.

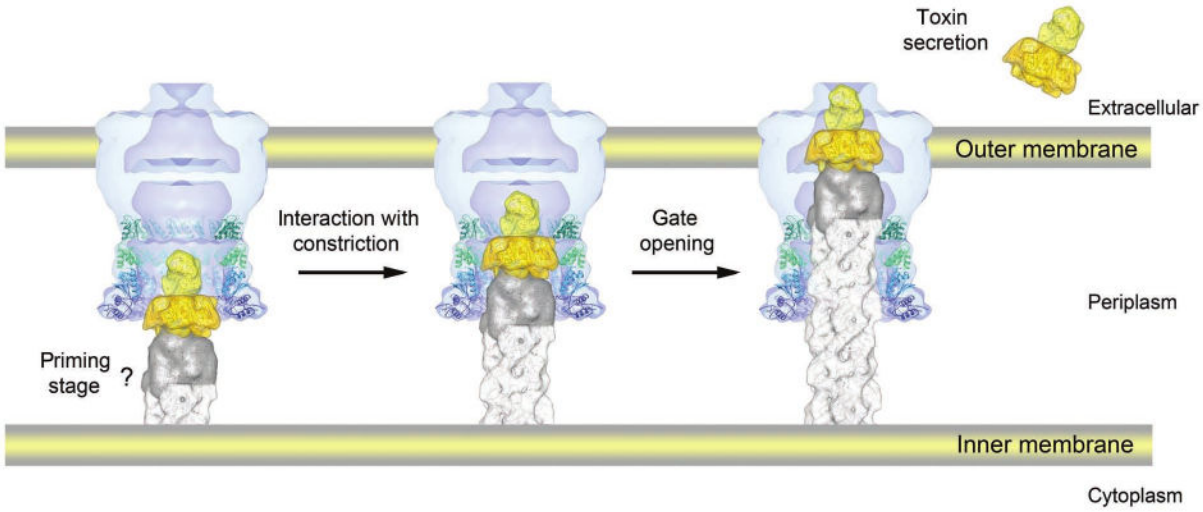

Figure 5. Piston driven mechanism for protein secretion

Illustration of key structural steps proposed to occur during protein secretion across the outer membrane by the type 2 secretion system. (*left*) The T2SS secretin (blue) is in its closed state. Large exoproteins, such as the cholera toxin AB_5 heterohexamer (gold), are proposed to interact with the pseudopilus tip complex (grey) positioned at the inner membrane beneath the secretin channel, or bind directly to the secretin. (*middle*) The pseudopilus would then extend acting like a piston to push the toxin into the periplasmic vestibule of the secretin and onto the constriction. (*right*) The interaction between the N3 domain (constriction) and large exoproteins like the toxin could act as the trigger to open the periplasmic gate, allowing exoproteins to enter the extracellular chamber of the secretin. The final step would involve opening of the extracellular gate, allowing exoproteins to be secreted (See also Discussion).